Analysis of Intrafractional Organ Motion by Megavoltage Computed Tomography in Patients with Lung Cancer Treated with Image-guided Stereotactic Body Radiotherapy Using Helical Tomotherapy

NORIHIRO AIBE[1,2], HIDEYA YAMAZAKI[1,2], TAKUYA NISHIMURA[1], YOSHITAKA OOTA[1], KAZUKI IWAMA[1], SATOAKI NAKAMURA[1,2], HIROYASU IKENO[2], KEN YOSHIDA[3] HARUUMI OKABE[1] and KEI YAMADA[2]

[1]Department of Radiology, Ujitakeda Hospital, Uji-city, Kyoto, Japan;
[2]Department of Radiology, Graduate School of Medical Science, Kyoto Prefectural University of Medicine, Kamigyo-ku, Kyoto, Japan;
[3]Department of Radiology, Osaka Medical College, Takatsuki City, Osaka, Japan

Abstract. *Aim: To analyze intrafractional organ motion in patients with lung cancer treated with image-guided stereotactic body radiotherapy using helical tomotherapy (SBRT-HT). Patients and Methods: Data from 25 patients with lung cancer who received 50 Gy/5 fractions of SBRT-HT were analyzed. Slow-scan megavoltage computed tomography (MVCT) images were acquired before (pre-MVCT) and after (post-MVCT) each fraction. We analyzed the imaging quality of the 124 post-MVCT images to identify tumor contours using low-density settings. Next we examined tumor contour deviations from the planning target volume (PTV) in post-MVCT images for intrafractional tumor displacement. Results: Image quality was determined as good in 111/124 images from 22 patients (92%). None of the upper lung tumor images were of poor quality (74 images in 15 patients), whereas lower lung tumors yielded 14 poor-quality images out of the 50 images (3/10 patients). The difference in image quality between upper and lower lung tumors was statistically significant ($p<0.01$), especially when accompanied by interstitial lung shadows. Deviations in tumor position in post-MVCT images were analyzed in 110 images from 23 patients and revealed 99 images (90%) with tumor contours confined to PTV. In upper lung tumors, 4/74 images in 15 patients (5.4%) showed tumor contour deviations outside PTV. Lower lung tumors showed a higher rate of deviation with 7/36 images in 8 patients (19.4%) showing tumor contour deviations outside PTV ($p<0.05$). The maximum deviation was 1 mm for upper lung tumors and 2 mm for lower lung tumors. Conclusion: Upper lung tumors are good candidates for MVCT image-guided SBRT-HT. However, lower lung tumors, especially those adjacent to the diaphragm or pleura, can be difficult to assess, warranting precise dose delivery by MVCT image-guided SBRT-HT.*

Radiotherapy is one of the most common treatments for localized lung cancer. The advent of the stereotactic body radiotherapy (SBRT) technique has made possible the delivery of higher doses of radiation without severe adverse reactions. Intensity-modulated radiotherapy (IMRT) allows the administration of higher radiation doses to the target while limiting the exposure of the surrounding normal organs (1). Image-guided radiotherapy (IGRT) is the use of 2-dimensional and 3-dimensional imaging during a radiotherapy course. This process uses imaging coordinates to accurately direct radiation to specific sites, allowing smaller set-up margins and decreasing the planned target volume (PTV) in lung cancer treatment (2). Helical tomotherapy is a form of IMRT that uses pre-treatment megavoltage computed tomography (MVCT) images of the patient in the treatment position. The precise positioning achieved by the use of MVCT images allows not only correct bone position (bone matching) as with conventional radiotherapy (3) but also visualization and identification of the precise location of lung tumors. Interfractional organ motion is, thus, negligible using this technique not requiring the use of invasive markers that can be a preferable treatment option, especially in elderly patients or those with a poor general condition. Several institutions, including ours, have

Correspondence to: Hideya Yamazaki, MD, Department of Radiology, Kyoto Prefectural University of Medicine, 465 Kajiicho Kawaramachi Hirokoji, Kamigyo-ku, Kyoto, Kyoto 602-8566, Japan. Tel: +81 752515618, Fax: +81 752515840, e-mail: hideya10@hotmail.com

Key Words: Tomotherapy, lung cancer, soft tissue matching, image-guided SBRT.

adopted the use of SBRT using helical tomotherapy (SBRT-HT) (4-10). The purpose of the present study was to verify the geometric accuracy of SBRT-HT by comparing tumor positions in kilovolt CT (kVCT) treatment-planning images and post-MVCT images. At first, we examined whether MVCT images are suitable for assessing lung tumor contours. Then, we determined whether tumors were located inside PTV or not, using only good-quality images.

Patients and Methods

Patients and tumor characteristics. Between March 2007 and February 2013, 25 lung tumors in 25 patients (18 males and 7 females) were treated with SBRT-HT (HI-ART TomoTherapy Inc., Madison, WI, USA). The ages of the patients ranged from 59 to 80 years (median=71 years). The pre-treatment characteristics of patients and tumors are summarized in Table I. All but 3 patients were pathologically diagnosed with lung cancer and considered medically inoperable because of chronic pulmonary or cardiovascular disease, advanced age or other complicating diseases. Three patients were clinically diagnosed without pathological diagnosis because they refused or had contraindications to pathologic diagnosis.

Treatment planning and dose delivery. All patients underwent 3 simulation CT scans (Aquilion 64 Toshiba Medical Co., Tokyo, Japan) in 3 phases, *i.e.*, free breathing, inhalation and exhalation, during shallow breathing. The gross tumor volume (GTV) in each phase was delineated using lung CT (window level, −550 HU Hounsfield unit (HU); width, 1600 HU) and a radiation treatment-contouring system (FocalPro version 4.50; FOCAL, ELEKTA AB, Stockholm, Sweden). GTVs for the 3 phases were fused and expanded as a PTV with a margin of 5-7 mm in the anterior-posterior and right-left directions (5 mm in most cases) and 5-10 mm in the superior–inferior and anterior–posterior direction (5 mm in most cases). The following structures were contoured as organs at risk: spinal cord, esophagus, lung and others as needed (*e.g.*, heart, ipsilateral bronchus, liver and bowel). The lung volume on the dose–volume histogram was defined as the value after the combined volume of the 3 respiration-phase GTVs was subtracted from the volume of the bilateral lungs. Treatment planning was performed using the Tomotherapy Hi-Art System workstation (HI-ART TomoTherapy Inc.). Treatment was generally delivered such that >95% of PTV received the prescribed dose of 50 Gy. All patients were immobilized in the supine position using the Body FIX® Vacuum Pump P2 system (Medical Intelligence, Schwabmünchen, Germany) and underwent MVCT for pretreatment set-up using the tomotherapy registration system. MVCT images (3.5 MV) were acquired through PTV before treatment delivery, with a minimum slice thickness of 4 mm and a field of view of 35 cm. Pre-MVCT images were autofused with the kVCT treatment-planning images; the superior–inferior, anterior–posterior and right–left shifts were then calculated by automatic image fusion for bone matching. Two clinicians manually inspected the fused images for tumor shadows for determining whether it was located within PTV. Rotational corrections were not implemented. Treatment was delivered after the patient and target were appropriately aligned 3-dimensionally using the checkerboard and partial transparent image overlay to confirm that the target was within PTV on the kVCT–MVCT fusion images. The center of mass of GTV could be identified in all pre-MVCT mages under several different conditions, if required, and adjustments could be made such that the motion-encoded target was in the center of PTV. We made an MVCT image just after treatment (post-MVCT) to confirm the tumor position. All patients provided written informed consent.

Table I. *Patients' characteristics*.

Variables		No. or median (range)
Gender	Male	18
	Female	7
Age		78.5 (63-87)
T category	T1a	17
	T1b	3
	T2a-	5
Histology	Adenocarcinoma	15
	Squamous cell carcinoma	5
	Non-squamous cell carcinoma	2
	NA	3
Gross tumor volume	(cm^3)	4.8 (1.0-33.4)
Planning target volume	(cm^3)	32 (10.1-120.8)

NA, Not available.

MVCT image quality analysis. We performed image quality analysis on post-MVCT images using a density setting; low density (window level=−600 HU, width=700 HU) according to the method of Smeenks (11). We classified the images according to quality as either good (clear borders in all directions) or poor (ambiguous border in at least 1 direction). Poor-quality images were not adequate to identify the tumor contours (Figure 1) (11).

Tumor deviation analysis. We analyzed contour deviations only in good-quality post-MVCT images that were made using the low-density setting. This setting is preferred because it reveals lung tumor contours more precisely in diagnostic CT images (11) (Figure 2). We determined whether the tumor contours were inside PTV and measured any deviations in 6 directions (superior–inferior, right–left, anterior–posterior).

Statistical analysis. All statistical analyses were performed using the Stat-view 5.0 statistical software (SAS Institute, Inc., Cary, NC, USA). Frequencies were analyzed using the χ^2 test. All analyses used the conventional $p<0.05$ level of significance.

Results

MVCT image quality analysis. Twenty-five patients were treated with 50 Gy/5 fractions. Out of the possible 125 fractions, 124 post-MVCT images were examined. One post-MVCT image was not obtained because the patient's condition did not permit post-MVCT on the 3rd day (PTID 13). Fourteen images in 3 patients were determined as poor-quality images under low-density conditions (Figure 1). We then categorized the tumors by location as either upper lung

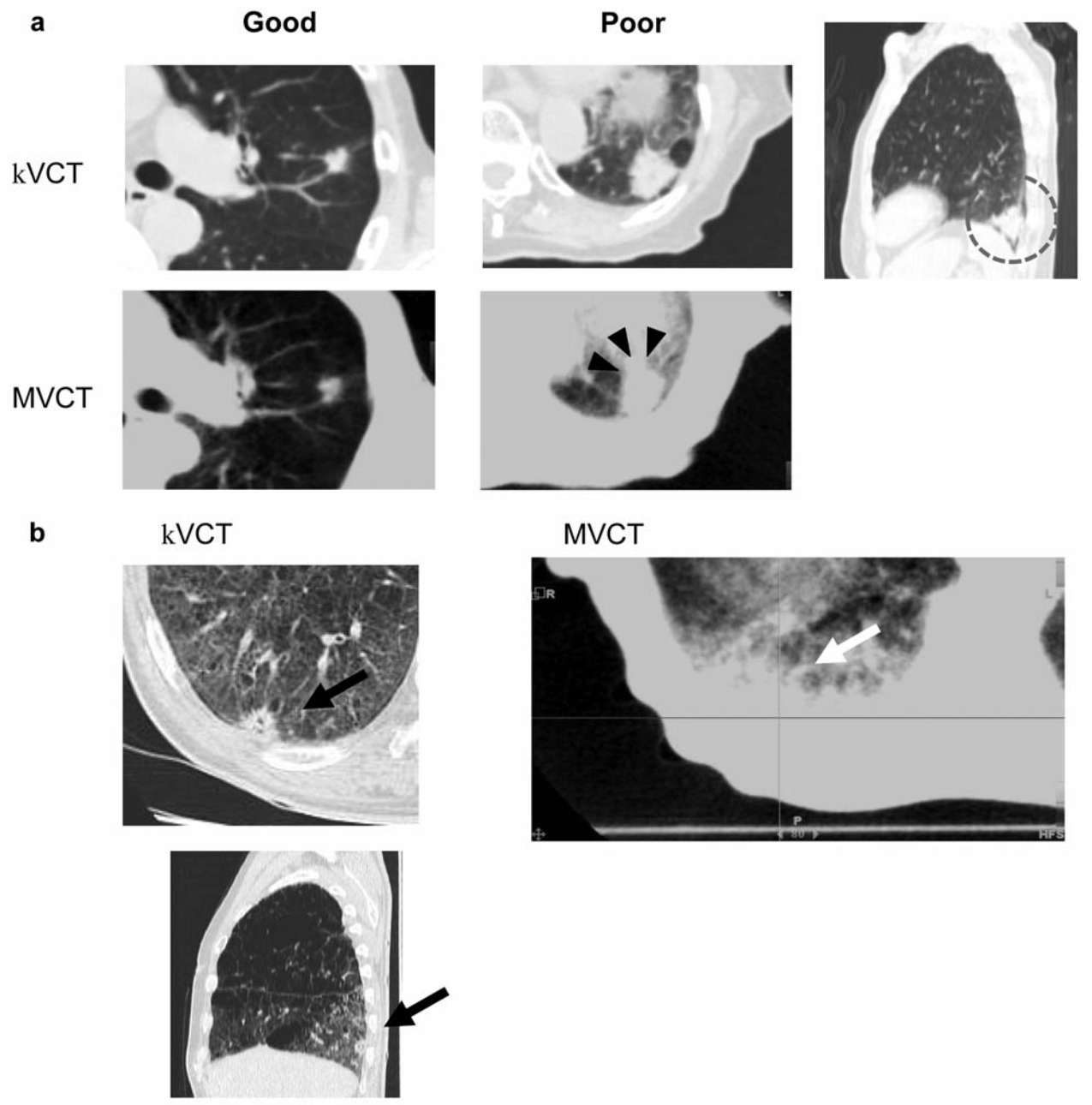

Figure 1. *Scheme of megavoltage computed tomographic (MVCT) image quality analysis. a) Left panel shows "good" quality image. Right panel shows "poor" image with ambiguous tumor contour caused by pleura/ diaphragm. b) Case of "poor" quality to analyze tumor contour. Note tumor contour ambiguity due to adjacent pleura and surrounding interstitial lung shadow.*

(upper lobe excluding the middle/ lingular segments) or lower lung (lower lobe and middle lobe/lingular segments). None of the upper lung tumor images were of poor quality (74 images in 15 patients), whereas lower lung tumors yielded 14 poor-quality images (in 3 patients) out of the 50 images (in 10 patients). The difference in image quality between upper and lower lung tumors was statistically significant ($p<0.01$). The poor-quality images were of lesions in the lower lung that were adjacent to the pleura or diaphragm, especially when accompanied by interstitial lung shadow. Therefore, we excluded those 14 images from subsequent data analysis.

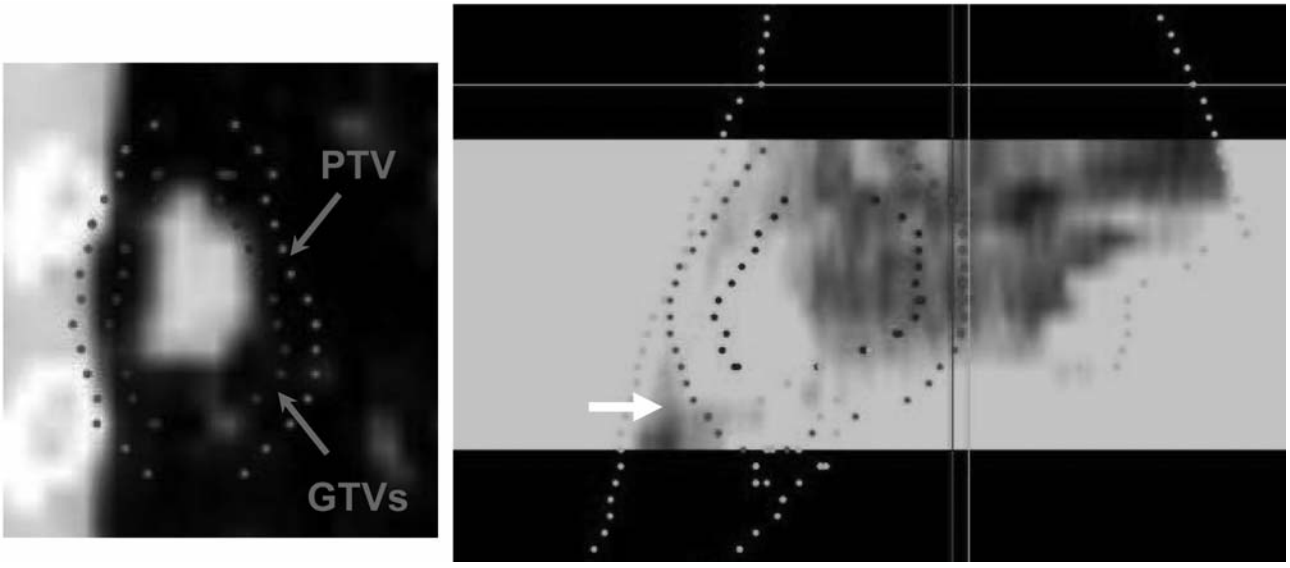

Figure 2. *Scheme of tumor deviation analysis using post-MVCT, sagittal scan. Case of contour deviation outside PTV into anterior caudal direction.*

Table II. *Deviation of tumor contours in post-treatment MVCT.*

	No. assessed images (No. PT)	Deviated cases (No. PT)	(%)	Involved cases (No. PT)	(%)	
Upper lung tumor	74 (15)	4 (1)	(5.4%)	70 (14)	(94.6%)	p<0.05 upper vs. lower lung tumor
Lower lung tumor	36 (8)	7 (4)	(19.4%)	29 (4)	(80.6%)	
Total	110 (23)	11 (5)	(10%)	99 (18)	(90%)	

MVCT, Megavoltage computed tomography; PT, patients.

Tumor deviation analysis using post-MVCT. We analyzed tumor contour deviations in 110 images from 23 patients that were determined to be of good quality in the low-density setting. Tumor contour deviations outside PTV were observed in 11 images (10%) from 5 patients (21%) (Table II) (Figure 2). Tumor contours were within PTV in 94.6% of upper lung tumors (70/74, from 15 patients) and 80.6% of lower lung tumors (29/36, from 8 patients) ($p<0.05$). Only 1 patient with an upper lung tumor (1/8; 87.5%) showed tumor contour deviations outside PTV, whereas 4 out of 8 patients (50%) with lower lung tumors showed tumor contour deviations outside PTV. The difference in tumor contour deviation rates between upper and lower lung tumors was statistically significant. The maximal deviations for 4 images of an upper lobe lesion (1 patient) were as follows: 1.0 mm in the right–left direction, 1.0 mm in the anterior–posterior direction and 0.5 mm in the superior–inferior direction. The corresponding values for 7 images of lower lobe lesions (4 patients) were as follows: 1.0 mm in the right–left direction, 2.0 mm in the anterior–posterior direction and 2.0 mm in the superior–inferior direction.

Discussion

Image-guided SBRT has been explored using several correctional strategies, including implanted fiducial markers and online 3-dimensional CT imaging (1, 12, 13). SBRT-HT with MVCT is a non-invasive image-guided SBRT and is feasible for use in elderly patients or those with a poor general condition or comorbidities. We have used SBRT-HT

and report preliminary good outcomes and toxicities (4). The quality of MVCT is an important consideration. Mahan *et al*. carried out anthropomorphic phantom studies that indicated MVCT images in tomotherapy were capable of sufficient accuracy to place the isocenter within 1 mm of the desired position (14). Because 1 gantry rotation takes 10 s in the MVCT imaging mode, MVCT images included motion-encoded treatment targets. Smeenks *et al*. have presented a phantom study for small moving objects on a helical MVCT scanner. Because a rapid MVCT scanner may be impractical because of engineering constraints, slow CT may be a viable alternative for some lung cancer patients treated with ungated tomotherapy, at the expense of increasing patient throughput (11).

Several authors have reported that image-guided IMRT has the potential to decrease PTV margins (7, 10, 13, 14). We have also investigated the required PTV margin in prostate cancer and a few vertebral body metastases using the van Herk's formula and found that 1-1.16 mm is sufficient to compensate for tumor displacement (3, 5). Using the formula proposed by van Herk *et al*. (2.5Ó + 0.7ó, where Σ and σ are systematic and random positioning errors, respectively) ensured that 90% patients receive a minimum cumulative CTV dose of at least 95% of the prescribed dose (15). Boggs *et al*. reported that the addition of a 7-mm margin to GTV for patients receiving SBRT for non-small cell lung cancers using tomotherapy is adequate to account for tumor displacement. Our results concur, suggesting that a 5-7 mm PTV margin may be sufficient to account for tumor displacement (3, 5, 16).

Waghorn *et al*. reported that targets moving >5 mm outside PTV can cause significant changes in target delivery, with the target delivery decreasing by up to 20% with target displacement 10 mm outside PTV margin; underdosing primarily limited to the target periphery (17). Margins several millimeters smaller than the maximum target displacement provided acceptable motion protection while also allowing for decreased exposure to normal tissues. Together, these results indicate that a tumor contour deviation of 1-2 mm outside PTV is small enough to warrant target dose coverage. However, we should keep in mind that lower lung tumors have greater ambiguity, warranting precise dose delivery by image-guided SBRT-HT if they are located adjacent to the diaphragm or pleural area, especially when accompanied with an interstitial lung shadow. Motion artifacts are observed more clearly in MVCT because this method uses a slow CT technique that reflects not only tumor motion but also the respiratory movement of adjacent structures. Therefore, for lower lung tumors, more precise estimation of the tumor margins (including the use of wider PTV margins, fiducial marking and real-time tracking) could be useful for maximizing the utility of imaging techniques.

In conclusion, upper lung tumors are good candidates for SBRT-HT. However, lower lung tumors adjacent to the diaphragm or pleural area, especially when with accompanied by interstitial lung shadow, are sometimes difficult to assess, warranting precise dose delivery by image-guided SBRT-HT.

Conflicts of Interest

None.

References

1 Glide-Hurst CK and Chetty IJ: Improving radiotherapy planning, delivery accuracy, and normal tissue sparing using cutting edge technologies. J Thorac Dis *6*: 303-318, 2014.

2 Thomsen MS, Harrov U, Fledelius W and Poulsen PR: Inter- and intra-fraction geometric errors in daily image-guided radiotherapy of free-breathing breast cancer patients measured with continuous portal imaging. Acta Oncol *53*: 802-808, 2014.

3 Nishimura T, Yamazaki H, Iwama K, Kotani T, Oota Y, Aibe H, Nakamura S, Ikeno H, Yoshida K, Isohashi F and Okabe H: Assessment of planning target volume margin for a small number of vertebral metastatic lesions using image-guided intensity-modulated radiation therapy by helical tomotherapy. Anticancer Res *33*: 2453-2456, 2013.

4 Aibe N, Yamazaki H, Nakamura S, Tsubokura T, Kobayashi K, Kodani N, Nishimura T, Okabe H and Yamada K: Outcome and toxicity of stereotactic body radiotherapy with helical tomotherapy for inoperable lung tumor: analysis of Grade 5 radiation pneumonitis. J Radiat Res *55*: 575-582, 2014.

5 Iwama K, Yamazaki H, Nishimura T, Oota Y, Aibe H, Nakamura S, Ikeno H, Yoshida K and Okabe H: Analysis of intrafractional organ motion for patients with prostate cancer using soft tissue matching image-guided intensity-modulated radiation therapy by helical tomotherapy. Anticancer Res *33*: 5675-5679, 2013.

6 Nishimura T, Yamazaki H, Iwama K, Kotani T, Oota Y, Aibe H, Nakamura S, Ikeno H, Yoshida K, Isohashi F and Okabe H. Assessment of planning target volume margin for a small number of vertebral metastatic lesions using image-guided intensity-modulated radiation therapy by helical tomotherapy. Anticancer Res *33*: 2453-2456, 2013.

7 Hodge W, Tome WA, Jaradat HA Orton NP, Khuntia D, Traynor A, Weigel T and Mehta MP: Feasibility report of image guided stereotactic body radiotherapy (IG-SBRT) with tomotherapy for early stage medically inoperable lung cancer using extreme hypofractionation. Acta Oncol *45*: 890-896, 2006.

8 Baisden JM, Romney DA, Reish AG Cai J, Sheng K, Jones DR, Benedict SH, Read PW and Larner JM: Dose as a function of lung volume and planned treatment volume in helical tomotherapy intensity-modulated radiation therapy-based stereotactic body radiation therapy for small lung tumors. Int J Radiat Oncol Biol Phys *68*: 1229-1237, 2007.

9 Tomita N, Kodaira T, Matsuo M, Furutani K, Tachibana H, Daimon T and Shimizu H: Helical tomotherapy for solitary lung tumor: feasibility study and dosimetric evaluation of treatment plans. Technol Cancer Res Treat *9*: 407-415, 2010.

10 Chi A, Jang SY, Welsh JS, Nguyen NP, Ong E, Gobar L and Komaki R: Feasibility of helical tomotherapy in stereotactic body radiation therapy for centrally located early stage nonsmall-cell lung cancer or lung metastases. Int J Radiat Oncol Biol Phys *81*: 856-862, 2011.
11 Smeenk C1, Gaede S and Battista JJ: Delineation of moving targets with slow MVCT scans: implications for adaptive non-gated lung tomotherapy. Phys Med Biol *52*: 1119-1134, 2007.
12 Chen J, Lee RJ, Handrahan D and Sause WT: Intensity modulated radiotherapy using implanted fiducial markers with daily portal imaging: assessment of prostate organ motion. Int J Radiat Oncol Biol Phys *68*: 912-919, 2007.
13 Cheng CW, Wong J, Grimm L, Chow M, Uematsu M and Fung A: Commissioning and clinical implementation of a sliding gantry CT scanner installed in an existing treatment room and early clinical experience for precise tumor localization. Am J Clin Oncol *126*: e28-36, 2003.
14 Mahan SL1, Ramsey CR, Scaperoth DD, Chase DJ and Byrne TE: Evaluation of image-guided helical tomotherapy for the retreatment of spinal metastasis. Int J Radiat Oncol Biol Phys *63*: 1576-1583, 2005.
15 van Herk M: Errors and margins in radiotherapy. Semin Radiat Oncol *14*: 52-64, 2004.
16 Boggs DH, Feigenberg S, Walter R, Wissing D, Patel B, Wu T and Rosen L: Stereotactic radiotherapy using tomotherapy for early-stage non-small cell lung carcinoma: Analysis of intrafraction tumour motion. J Med Imaging Radiat Oncol (in press).
17 Waghorn BJ, Shah AP, Rineer JM, Langen KM and Meeks SL: A margin-based analysis of the dosimetric impact of motion on step-and-shoot IMRT lung plans. Radiat Oncol *9*: 46, 2014.

Received August 11, 2014
Revised September 9, 2014
Accepted September 15, 2014